mathematics

MDPI

Article

A Synthetic Contact-Network Simulation Framework for Infection Risk and Appointment Control in Outpatient Care Facilities

Rong Fu [1,2], Ziyu Zhou [1], Hong Jiang [3] and Yunhe Tong [1,*]

[1] School of Resources and Safety Engineering, Central South University, Changsha 410083, China; rongfu0421@163.com (R.F.)
[2] Faculty of Health and Life Sciences, University of Bristol, Bristol BS8 1QU, UK
[3] College of Arts and Sciences, University of Cincinnati, Cincinnati, OH 45221, USA
* Correspondence: yunhetong@csu.edu.cn

Abstract

Outpatient care facilities combine high patient turnover, repeated short contacts, accompanying persons, clinically vulnerable subgroups, and healthcare-worker movement across functional zones. This study develops a synthetic dynamic contact-network simulation framework to evaluate how outpatient flow-control strategies affect simulated respiratory-infection risk and service efficiency. Public descriptions of the SocioPatterns hospital-ward study were used only to shape role composition and qualitative contact heterogeneity. A parameterized outpatient process model generated time-stamped locations for patients, accompanying persons, high-risk patients, and healthcare workers over a simulated clinic day. Zone- and role-dependent temporal contacts were then coupled to a stochastic SEIR process, with 500 replications per main scenario. In the baseline scenario, mean cumulative secondary infections were 0.502 per clinic day, the probability of at least one secondary infection was 0.354, and mean waiting time was 23.1 min. Time-spaced appointments reduced mean secondary infections by 45.4–52.2% while also reducing waiting time. Accompaniment restriction reduced risk by removing non-service nodes, whereas waiting-capacity control, protected scheduling, and healthcare-worker grouping were more context dependent. The strongest combined strategy reduced mean secondary infections by 52.6% and maintained a mean waiting time of 13.6 min. These results are comparative outputs under stated assumptions, not predictions for a specific clinic. The framework provides a reproducible computational basis for testing how operational policies reshape temporal contact opportunities before local implementation.

Keywords: epidemic modelling; dynamic contact network; SEIR model; outpatient care; appointment scheduling; infection control; healthcare operations; stochastic simulation

MSC: 05C82; 60J22; 90B22

Check for updates

Academic Editor: Liang Zhang

Received: 14 July 2026
Revised: 15 August 2026
Accepted: 18 August 2026
Published: 21 August 2026

1. Introduction

Outpatient care facilities are increasingly important sites of healthcare delivery. They include general outpatient clinics, specialist consultation clinics, infusion centres, oncology day-care units, diagnostic sampling areas, and follow-up services. Unlike inpatient wards, these environments are characterized by continuous inflow and outflow. Patients may arrive in concentrated waves, wait in shared spaces, move between consultation and treatment zones, and leave after a relatively short visit. Accompanying persons may remain with patients for part or all of the visit. Healthcare workers may interact with many patients in a single day and may move between consultation rooms, treatment areas, waiting spaces, entry points, and administrative zones. These features create a temporal contact system in which infection risk is shaped not only by pathogen biology, but also by the organization of patient flow.

Infection prevention in healthcare settings is commonly addressed through hand hygiene, respiratory etiquette, isolation precautions, environmental cleaning, screening, injection safety, and use of personal protective equipment. These practices remain essential and are central to current infection-prevention guidance for healthcare and outpatient settings [1–3]. However, operational organization can also affect transmission opportunities. Appointment timing determines how many people occupy waiting areas at the same time. Waiting-capacity policies determine whether patients are concentrated in one shared space or redistributed across time and space. Accompaniment policies change the number of nodes in the contact network. High-risk patient scheduling changes whether clinically vulnerable patients are mixed with general patients during peak periods. Healthcare-worker grouping changes whether staff act as bridges across otherwise separated patient groups. These operational mechanisms are not substitutes for infection-control standards, but they are mathematically meaningful because they reshape the dynamic network in which transmission can occur.

Classical compartmental epidemic models, including the SIR and SEIR families, provide the foundation for mathematical epidemic modelling [4]. These models are valuable because they translate transmission, latency, infectiousness, and removal into explicit dynamical equations. However, their common homogeneous-mixing form assumes that individuals experience the same effective contact rate within a population. This assumption is often too coarse for healthcare environments, where contacts are role-dependent, zone-dependent, and time-dependent. Network-based epidemic modelling addresses this limitation by representing heterogeneity in who contacts whom and how strongly individuals are connected [5–7]. Temporal-network approaches further extend this logic by representing contacts as time-indexed events rather than static links [8].

High-resolution contact studies show why temporal structure matters for infection modelling. Wearable sensors, RFID systems, and proximity-based data have revealed heterogeneous contact durations, repeated encounters, role-specific mixing, and high-contact individuals in schools, conferences, hospitals, and other social settings [9–15]. In hospital settings, proximity-sensor studies have shown that patients, healthcare workers, and administrative staff do not mix uniformly, and that a small number of healthcare workers may account for a large share of patient-related contacts [12,16]. These findings are important for outpatient modelling because outpatient facilities also contain heterogeneous roles, repeated short contacts, patient–staff interactions, and movement across functional zones.

Recent modelling studies have further highlighted the need to represent healthcare transmission through individual-level contact processes. During the COVID-19 pandemic, mathematical models were used to assess nosocomial transmission, healthcare-worker screening, personal protective equipment, contact tracing, staff cohorting, and patient contact networks [17–19]. Systematic reviews of outbreak models also show that network-based and stochastic models are increasingly used to represent spatial and temporal heterogeneity, although many studies still rely on synthetic or aggregated data when individual movement or contact data are unavailable [19,20]. These developments support the use of dynamic contact networks as a modelling bridge between healthcare operations and infection-risk analysis.

https://doi.org/10.3390/math14163021

Related literature in healthcare operations has examined outpatient appointment scheduling, waiting time, congestion, and service performance. Foundational reviews and later optimization studies show that outpatient appointment systems must balance patient waiting, provider idle time, resource use, demand uncertainty, no-shows, service-time variability, and operational constraints [21–23]. More recent work has emphasized that appointment scheduling in real outpatient clinics is not only a mathematical slot-allocation problem, but also a practical operations problem involving process variability, clinical priorities, resource constraints, and patient experience [24,25]. However, this literature usually evaluates efficiency outcomes rather than infection risk, whereas temporal contact-network models usually evaluate transmission mechanisms rather than outpatient service performance.

The modelling gap addressed in this study lies at the interface of outpatient operations and temporal-network epidemiology. Prior healthcare temporal-network SEIR studies primarily use observed or reconstructed patient–staff contacts to evaluate transmission control, whereas appointment-scheduling studies primarily optimize waiting, utilization, or access. The present framework differs by making the operational policy itself an upstream network-generating mechanism: arrival schedules, accompaniment, waiting-capacity rules, protected pathways, and staff assignments first alter time-stamped zone occupancy and contacts, after which transmission is simulated on the resulting network. The contribution is therefore a computational coupling of process simulation, policy-dependent temporal-network generation, stochastic SEIR transmission, and joint risk–efficiency evaluation; it is not a new SEIR theorem or a validated clinical forecasting model.

The novelty of this work is the integration of four components that are usually treated separately: outpatient process simulation, dynamic contact-network generation, stochastic temporal-network SEIR transmission, and operational risk–efficiency comparison. The study does not claim novelty in SEIR modelling alone, appointment scheduling alone, or contact-network analysis alone. Instead, its contribution is to combine these elements into a transparent simulation framework in which outpatient policies can be evaluated as network-shaping interventions. In this framework, an outpatient policy is not only an administrative rule; it is also a mechanism that changes who can meet whom, where contacts occur, and how long contact opportunities last.

The present study applies this framework to a simulated outpatient facility. Public hospital-ward descriptions provide qualitative constraints, but every calibration record used here is synthetically generated. The workflow then links five modules: synthetic contact constraints, outpatient trajectories, time-stamped weighted contacts, stochastic SEIR transmission, and comparative policy outcomes. The aim is not to forecast an outbreak in a named hospital. The public healthcare contact information used here comes from a hospital ward rather than an outpatient clinic [12]. Moreover, the raw temporal contact file was not accessible in the present execution environment. Therefore, the empirical component in the current version is implemented as a synthetic calibration dataset explicitly labelled as non-observed. The results should be interpreted as scenario-based simulation outputs under stated assumptions, not as observed hospital outcomes or direct clinical predictions.

The study is organized around three research questions. First, how does outpatient process organization shape the structure and intensity of dynamic contact networks? Second, how do appointment spacing, waiting-capacity control, accompaniment restriction, high-risk patient scheduling, healthcare-worker grouping, and combined strategies affect simulated respiratory infection transmission? Third, what trade-offs emerge between infection-risk reduction and service efficiency, measured by waiting time, patient sojourn time, waiting occupancy, and healthcare-worker utilization? By addressing these questions,

https://doi.org/10.3390/math14163021

the study provides a reproducible mathematical framework for evaluating outpatient infection-control strategies before local implementation.

2. Materials and Methods

This section defines the simulation population and time scale, explains the synthetic contact constraints and outpatient process, specifies temporal-network and SEIR equations with units, and describes intervention scenarios, replications, outcome definitions, and sensitivity analyses.

2.1. Study Design and Modelling Overview

This study used a synthetic, scenario-based simulation design to evaluate how outpatient flow organization may affect simulated infection risk and service efficiency. The model was not intended to predict infections in a specific clinic. Public healthcare-contact descriptions shaped qualitative structural constraints only; all calibration records used by the model were generated synthetically.

The modelling workflow consisted of five linked modules shown in Figure 1. Synthetic healthcare-contact constraints shaped role-specific heterogeneity; the outpatient process generated time-stamped zone trajectories; co-location produced weighted temporal contacts; a stochastic SEIR process operated on those contacts; and intervention scenarios were compared using infection, network, and service outcomes.

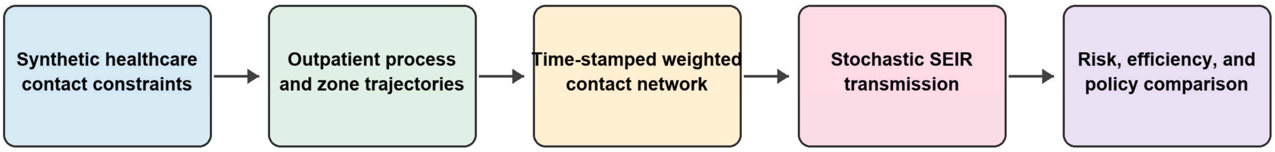

Figure 1. Computational workflow. Operational policies alter patient and staff trajectories and therefore the temporal contact network on which transmission is simulated. Baseline parameters are listed in Table 1.

Table 1. Model parameters and baseline values.

Parameter	Symbol	Baseline Value	Sensitivity Range	Source or Rationale
Outpatient patients per simulated day	N_p	80	80–160	Scenario assumption
Healthcare workers	N_h	8	8–16	Scenario assumption
High-risk patient fraction	q_h	0.20	0.10–0.30	Clinical scenario assumption
Time step	Δt	5 min	5–10 min	Temporal network resolution
Clinic day	T	480 min	360–540 min	One outpatient day
Transmission rate	β	0.0135 min^{-1}	0.007–0.027 min^{-1}	Generic respiratory-infection scenario; not fitted
Initial infectious individuals	I_0	3	1–5	Imported infection scenario
Main replications	R	500	LHS: 100	Main scenario outcomes used 500 replications; global sensitivity used 512 LHS points with 100 replications per point
Baseline accompaniment	p_a	0.80	0–1	Policy variable
Waiting capacity	k_w	No limit	20–50	Policy variable

https://doi.org/10.3390/math14163021

Table 1. *Cont.*

Parameter	Symbol	Baseline Value	Sensitivity Range	Source or Rationale
Mean latent period	$1/\sigma$	2 days (σ = 0.001735 per 5 min)	1–4 days	Generic scenario assumption
Mean infectious period	$1/\gamma$	5 days (γ = 0.000694 per 5 min)	3–8 days	Generic scenario assumption

The unit of analysis was one outpatient facility over a working day of 480 min. The temporal resolution was 5 min. This interval was selected to represent movement between outpatient zones while keeping stochastic replications computationally tractable. Each scenario included 80 patients and 8 healthcare workers. Twenty percent of patients were designated as high risk. High-risk status represented a generic clinically vulnerable outpatient subgroup, such as oncology patients, immunosuppressed patients, frail older patients, or patients requiring longer treatment. The model did not assume that cancer or any other non-infectious condition is transmissible. The transmissible process was a generic respiratory infection. The main model parameters and baseline values are summarized in Table 1.

2.2. Synthetic Contact Calibration Informed by Public Healthcare Contact Data

The intended empirical calibration source was the SocioPatterns hospital-ward dynamic contact network. Public documentation describes this dataset as a temporal contact network recorded in a hospital ward in Lyon, France, from 6 December 2010 at 13:00 to 10 December 2010 at 14:00. It includes contacts among patients, between patients and healthcare workers, and among healthcare workers, with 46 healthcare workers and 29 patients recorded at 20 s contact intervals.

The raw temporal contact file was not accessed or processed in this study. Accordingly, "synthetic" means that all pairwise records were generated by the model; "public-data-shaped" means only that publicly reported role composition and qualitative properties of the SocioPatterns hospital study motivated constraints on role mixing, right-skewed durations, and high-contact individuals. No numeric contact distribution, outpatient layout, or disease parameter was estimated from the French ward data. This terminology prevents the simulated calibration from being interpreted as empirical validation.

The calibration data were used only to inform contact heterogeneity in the outpatient simulation. They were not used to estimate disease-specific transmission parameters and should not be interpreted as observed outpatient contact data. The accompanying code was organized so that the synthetic generator can be replaced by a raw temporal contact file when such data are available.

From the calibration dataset, the following quantities were computed: pairwise contact duration, individual total contact duration, number of distinct contacts per individual, role-specific mixing matrix, weighted degree distribution, and the cumulative concentration of contact duration among ranked individuals. These quantities were used to guide role-informed contact-duration sampling in the outpatient contact-network simulation.

2.3. Outpatient Process Simulation

The outpatient process model generated the location history of each individual over the simulated clinic day. Patients moved through a simplified outpatient pathway consisting of entry and screening, waiting, consultation, treatment or examination if required, and exit. Some patients required only consultation, whereas others required treatment or examination after consultation. High-risk patients were assigned a higher probability of requiring treatment and longer treatment duration, reflecting the possibility that clinically vulnerable patients may have more complex visits.

Accompanying persons followed the associated patient unless the scenario restricted accompaniment. They did not receive medical service, but they contributed additional nodes and potential contacts to the network. Healthcare workers were assigned to entry, waiting, consultation, treatment, or exit-related zones. Under normal staffing, some healthcare workers could move between zones. Under the grouped staffing scenario, healthcare workers were more strongly assigned to fixed zones to represent reduced cross-zone movement.

Arrival patterns varied by scenario. The baseline concentrated arrivals early in the clinic day, whereas appointment-spacing scenarios distributed arrivals over longer windows. Service durations were sampled from gamma or triangular scenario distributions. Waiting-capacity control did not remove patients; excess patients were routed to a lower-contact buffer representing pre-entry, external, or physically separated waiting. Consequently, a capacity limit can redistribute rather than eliminate contacts. A real implementation should specify whether the buffer is physically separated, ventilated, supervised, and compatible with priority or fast-track pathways.

2.4. Dynamic Contact-Network Construction

Let $V = \{1, 2, \ldots, N\}$ denote the set of individuals present in a scenario. At each time step t, each individual had either a zone label or no active location if not present in the facility. A temporal contact could occur only when two individuals were present in the same zone during the same time interval.

For a zone r, let $n_r(t)$ denote the number of individuals present in that zone at time t. The number of possible dyads in that zone was

$$Dr(t) = n_r(t)[n_r(t) - 1]/2$$

A binomial draw was used to determine how many dyads formed contacts during the time interval:

$$C_r(t) \sim Binomial(D_r(t), p_r)$$

where p_r is the zone-specific contact probability. Entry and exit zones were assigned lower contact probabilities, waiting and treatment zones were assigned higher probabilities, and consultation represented the highest-intensity clinical-contact zone. Contact dyads were then sampled from the possible within-zone dyads.

Each temporal contact was represented as a weighted edge $e_{ij}(t)$ between individuals i and j. The edge weight $w_{ij}(t)$ is defined exclusively as contact duration in minutes accrued within the 5 min interval; it is not a dimensionless intensity. Role-informed lognormal draws were truncated at 5 min so that $0 \leq w_{ij}(t) \leq 5$ min. Aggregated network outcomes included total contact-minutes, mean weighted degree in contact-minutes per person, network density, role mixing, waiting- and treatment-zone contact burden, high-contact-node contribution, and the healthcare-worker bridge index.

The healthcare-worker bridge index was defined as the proportion of healthcare-worker contact duration that connected healthcare workers to non-healthcare-worker nodes. It was not intended as a formal graph-theoretic betweenness measure. Rather, it served as an operational indicator of the extent to which healthcare workers connected patient and accompanying-person groups through repeated cross-role service contacts.

2.5. Stochastic SEIR Transmission Model on Temporal Networks

A stochastic SEIR process was simulated on each dynamic contact network. Each individual was assigned one of four states: susceptible S, exposed E, infectious I, or removed R. At each time step, susceptible individuals could become exposed through contact with infectious individuals.

If susceptible individual i contacted infectious individual j during time interval t, the infection probability was

$$p_{ij}(t) = 1 - exp\left[-\beta w_{ij}(t)\right]$$

where β = 0.0135 min^{-1} is the transmission hazard per contact-minute and $w_{ij}(t)$ is contact duration in minutes. Thus, $\beta w_{ij}(t)$ is dimensionless. The value is a generic respiratory-infection scenario parameter used for comparative analysis, not an estimate from the synthetic contact data or a calibrated pathogen-specific value.

$$p_i(t) = 1 - \prod_{j \in I(t)} \left[1 - p_{ij}(t)\right]$$

Exposed individuals became infectious with per-step probability σ = 1 − exp[−Δt/(2 days)] = 0.001735 for Δt = 5 min, and infectious individuals moved to the removed state with probability γ = 1 − exp[-Δt/(5 days)] = 0.000694. These illustrative mean latent and infectious periods were held constant across scenarios. Because the horizon is one clinic day, the main endpoint is the number of susceptible individuals newly entering E, rather than long-term epidemic size.

The baseline transmission rate was β = 0.0135 min^{-1}, with three infectious individuals introduced at opening. Parameter values were selected as transparent generic scenario assumptions or operational policy variables rather than fitted estimates. Table 1 now states the source or rationale for every baseline value; β, σ, and γ were varied or interpreted cautiously because the framework is not pathogen-calibrated.

2.6. Intervention Scenarios

Intervention scenarios were designed to compare operational policies that could plausibly be adjusted in outpatient facilities. The baseline scenario combined concentrated arrivals, no waiting-capacity control, 80% accompaniment probability, mixed scheduling of high-risk patients, and normal healthcare-worker movement.

Appointment-spacing scenarios used distributed arrival schedules labelled Appt-10min, Appt-20min, and Appt-30min. Capacity scenarios restricted the main waiting area to 50 or 30 individuals. Accompaniment scenarios reduced accompaniment probability to 0% or 30%. The protected high-risk scenario assigned high-risk patients to an early protected block. The healthcare-worker grouping scenario reduced cross-zone staff movement. Two combined scenarios were also tested. Combined-A used time-spaced appointments with 30% accompaniment. Combined-B combined time-spaced appointments, waiting capacity of 30, 30% accompaniment, protected high-risk scheduling, and healthcare-worker grouping.

The protected high-risk scenario was interpreted cautiously. In real outpatient settings, protected scheduling may be implemented as a low-density appointment block, a physically separated patient stream, or a priority fast-track pathway. In the present simplified model, protected scheduling mainly shifted high-risk patients into an early block. This design could reduce mixing with the general patient population, but it could also create local concentration if not paired with density control. The scenario therefore tested whether separation alone was sufficient, rather than assuming that any protected block would necessarily reduce risk. The intervention scenarios are summarized in Table 2.

Table 2. Intervention scenarios.

Scenario	Appointment Rule	Waiting Capacity	Accompaniment Policy	High-Risk Scheduling	HCW Grouping
Baseline	concentrated	No limit	80%	Mixed	Normal
Appt-10min	spread10	No limit	80%	Mixed	Normal
Appt-20min	spread20	No limit	80%	Mixed	Normal
Appt-30min	spread30	No limit	80%	Mixed	Normal
Capacity-50	concentrated	50	80%	Mixed	Normal
Capacity-30	concentrated	30	80%	Mixed	Normal
Accomp-0	concentrated	No limit	0%	Mixed	Normal
Accomp-30	concentrated	No limit	30%	Mixed	Normal
HighRisk-Protected	concentrated	No limit	80%	Protected	Normal
HCW-Grouped	concentrated	No limit	80%	Mixed	Grouped
Combined-A	spread20	No limit	30%	Mixed	Normal
Combined-B	spread20	30	30%	Protected	Grouped

2.7. Replications, Uncertainty, and Outcome Metrics

Main scenario outcomes were estimated using 500 independent stochastic replications per scenario. The multivariable global sensitivity analysis used 512 Latin hypercube design points and 100 stochastic epidemic replications per point, producing 51,200 replicate-level outputs. Each LHS point used one operational process and contact-network realization, followed by 100 epidemic replications on that network. Simulation ranges describe stochastic model output and are not confidence intervals from clinical observations.

"Cumulative secondary infections" denotes the number of initially susceptible individuals who entered the exposed state during the simulated clinic day. "Probability of any secondary infection" is the fraction of replications with at least one such event. The "scenario reproduction proxy" is mean secondary infections divided by the three initially infectious individuals; it is not R0 or an epidemic reproduction number. "High-contact-node contribution" is the share of total contact-minutes accumulated by the highest-contact decile of nodes. Service outcomes include mean, median, and 95th-percentile waiting time, peak waiting occupancy, mean sojourn time, healthcare-worker utilization, and completed patients.

An illustrative composite score J was computed only as a decision-aid visualization. Cumulative infections I and mean waiting time T were min–max normalized: X~ = (X − Xmin)/(Xmax − Xmin). Control burden C was the number of active intervention components (appointment spacing, capacity control, accompaniment restriction, protected scheduling, and healthcare-worker grouping) divided by five. The plotted score used equal weights w1 = w2 = w3 = 1/3:

$$J = w_1\tilde{I} + w_2\tilde{T} + w_3\tilde{C}$$

where the three normalized terms lie in [0, 1]. Equal weights are not asserted to represent universal stakeholder preferences. Weight checks that prioritize infection risk, waiting time, or control burden should therefore accompany local use; the unaggregated outcomes remain the primary evidence whenever rankings change with weights.

2.8. Multivariable Global Sensitivity Analysis

A randomized Latin hypercube sampling design was used to evaluate epidemiological and operational uncertainty simultaneously. The design jointly varied the transmission rate β from 0.007 to 0.027 min^{-1}, initial infectious count from 1 to 5, accompaniment probability from 0 to 1, waiting capacity from 20 to 50 persons, and contact scaling from 0.75 to 1.25. The four archived arrival schedules, concentrated, spread10, spread20, and spread30, were equally represented, with 128 design points assigned to each schedule.

An interaction-aware response surface was fitted to design-point means. The model included numeric main effects, quadratic terms, all pairwise numeric interactions, arrival-schedule indicators and interactions of arrival schedule with β, accompaniment probability, and waiting capacity. The prespecified interaction of primary interest was β × waiting capacity. Bootstrap intervals were calculated by resampling the 512 design points. The fixed seeds were 20,260,815 for the LHS design, 20,260,708 for the archived simulation model, and 20,260,816 for bootstrap resampling.

3. Results

3.1. Calibration-Derived Contact Heterogeneity and Outpatient Contact-Network Formation

To evaluate whether the simulated outpatient contact networks contained the heterogeneity required for temporal-network epidemic modelling, we first examined the synthetic healthcare-contact calibration outputs. This step was necessary because outpatient transmission risk is shaped not only by the number of people in the facility, but also by role-specific mixing, contact duration, repeated encounters, and the extent to which a small number of individuals accumulate a large share of total contact time.

The synthetic calibration reproduced key features needed for contact-network simulation without presenting itself as observed outpatient data. Figure 2A shows that contact duration was unevenly distributed across patient and healthcare-worker role classes. Figure 2B shows a right-skewed distribution of pairwise contact durations, with many short contacts and fewer longer contacts. Figure 2C further indicates that contact duration varied across patient–patient, patient–healthcare-worker, and healthcare-worker–healthcare-worker pairs. At the individual level, Figure 2D shows substantial variation in accumulated contact burden within roles, while Figure 2E indicates that individuals with more distinct contacts tended to accumulate longer total contact durations.

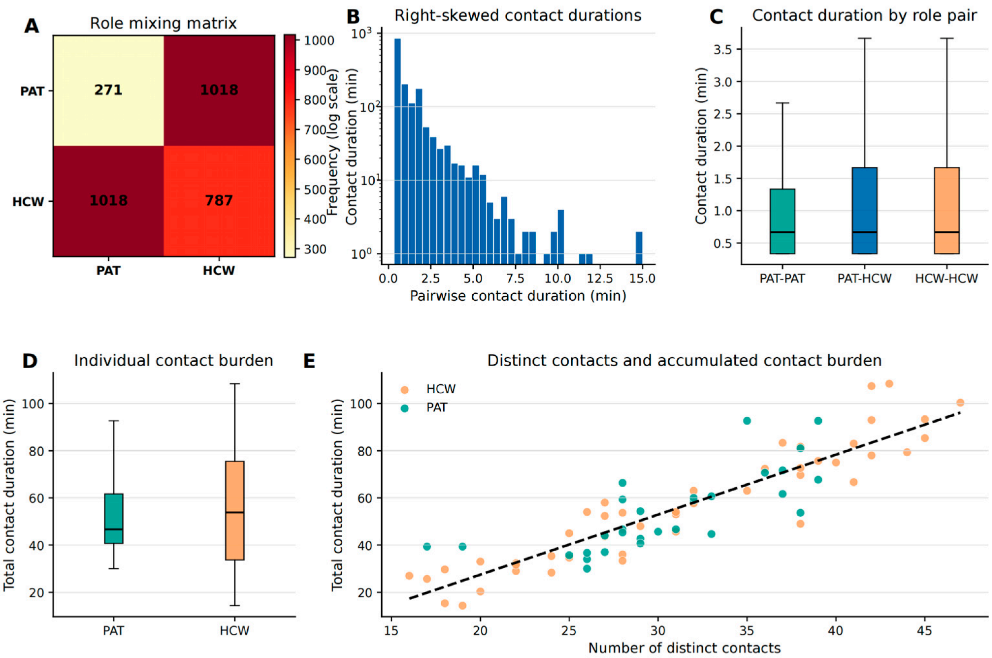

Figure 2. Calibration-derived contact heterogeneity in the synthetic, non-observed healthcare contact network. (**A**) Role-specific contact mixing matrix. (**B**) Distribution of pairwise contact durations. (**C**) Pairwise durations by role pair. (**D**) Individual contact burden by role. (**E**) Distinct contacts versus accumulated duration. Synthetic generator settings are described in Section 2.2.

These calibration results were not used to estimate pathogen-specific transmission parameters. Instead, they were used to inform the heterogeneity of temporal contact durations and the possibility that a minority of individuals can contribute disproportionately to contact burden. This distinction is important because the public SocioPatterns dataset used for calibration context is a hospital-ward dataset rather than an outpatient clinic dataset. The calibration therefore constrains plausible healthcare contact heterogeneity but does not empirically represent outpatient flow.

The outpatient process simulation then translated appointment rules, waiting behaviour, accompaniment, high-risk scheduling, and healthcare-worker movement into temporal contact networks. Under the baseline scenario, the outpatient process generated 1446 temporal contacts and a mean weighted degree of 14.48 contact-minutes per person. Peak waiting occupancy was 48, indicating that concentrated arrivals created a substantial waiting-room contact burden.

Appointment spacing reshaped the contact network before any transmission process was simulated. Appt-10min reduced total temporal contacts to 656, and Appt-20min reduced them to 635. Mean weighted degree decreased from 14.48 under baseline to 6.18 and 5.97, respectively. Peak waiting occupancy also decreased from 48 under baseline to 9 under Appt-10min and 14 under Appt-20min. These results show that appointment organization reduced contact intensity primarily by flattening crowding peaks.

Accompaniment restriction also reduced contact opportunities by decreasing the number of non-service nodes in the facility. With no accompaniment, total temporal contacts decreased to 661; with 30% accompaniment, the value was 815. This supports the interpretation that accompanying persons can increase contact-network size and contact burden even though they do not receive medical services. Healthcare-worker grouping had a weaker structural effect in this parameterization. The healthcare-worker bridge index was 0.746 under baseline and 0.785 under grouped work, suggesting that grouping alone did not remove cross-role contacts because healthcare workers still needed to serve patients. Overall, appointment spacing and accompaniment control acted directly on the temporal contact structure, whereas the effect of staff grouping depended more strongly on how clinical work was organized.

As a structural benchmark, the baseline network was also compared with a contact-matched homogeneous-mixing approximation using the same β, three initial infectious individuals, an expected baseline population of 152 (80 patients, 8 healthcare workers, and 64 accompanying persons), and the observed baseline mean weighted degree of 14.48 contact-minutes per person. Randomly redistributing the same aggregate contact-minutes gives an analytical expectation of approximately 0.58 secondary infections, compared with 0.502 in the temporal-network simulation. The homogeneous approximation is therefore useful as a scale check but cannot identify role-, zone-, or timing-specific pathways or reproduce policy effects that act by rearranging contacts.

3.2. Operational Flow-Control Effects on Infection Risk and Service Efficiency

To assess whether operational flow control could reduce infection risk while maintaining service efficiency, appointment spacing, waiting-capacity control, and accompaniment restriction were compared using the stochastic temporal-network SEIR model. These policies were selected because they can often be adjusted at the level of clinic operations without changing the medical treatment itself. Infection outcomes were therefore evaluated together with waiting-time outcomes, since a policy that reduces contact opportunities may still be undesirable if it substantially increases patient delay or shifts crowding to another zone.

Appointment spacing produced the clearest improvement among the single operational strategies. In the baseline scenario, cumulative secondary infections averaged 0.502 per clinic day, and the probability of any secondary infection was 0.354. Appt-10min and Appt-20min both reduced mean cumulative secondary infections to 0.240, corresponding to reductions of 52.2% relative to baseline. Appt-30min reduced mean cumulative secondary infections to 0.274, a reduction of 45.4%. Figure 3A shows the mean secondary infections across scenarios, and Figure 3C shows the corresponding reduction relative to baseline.

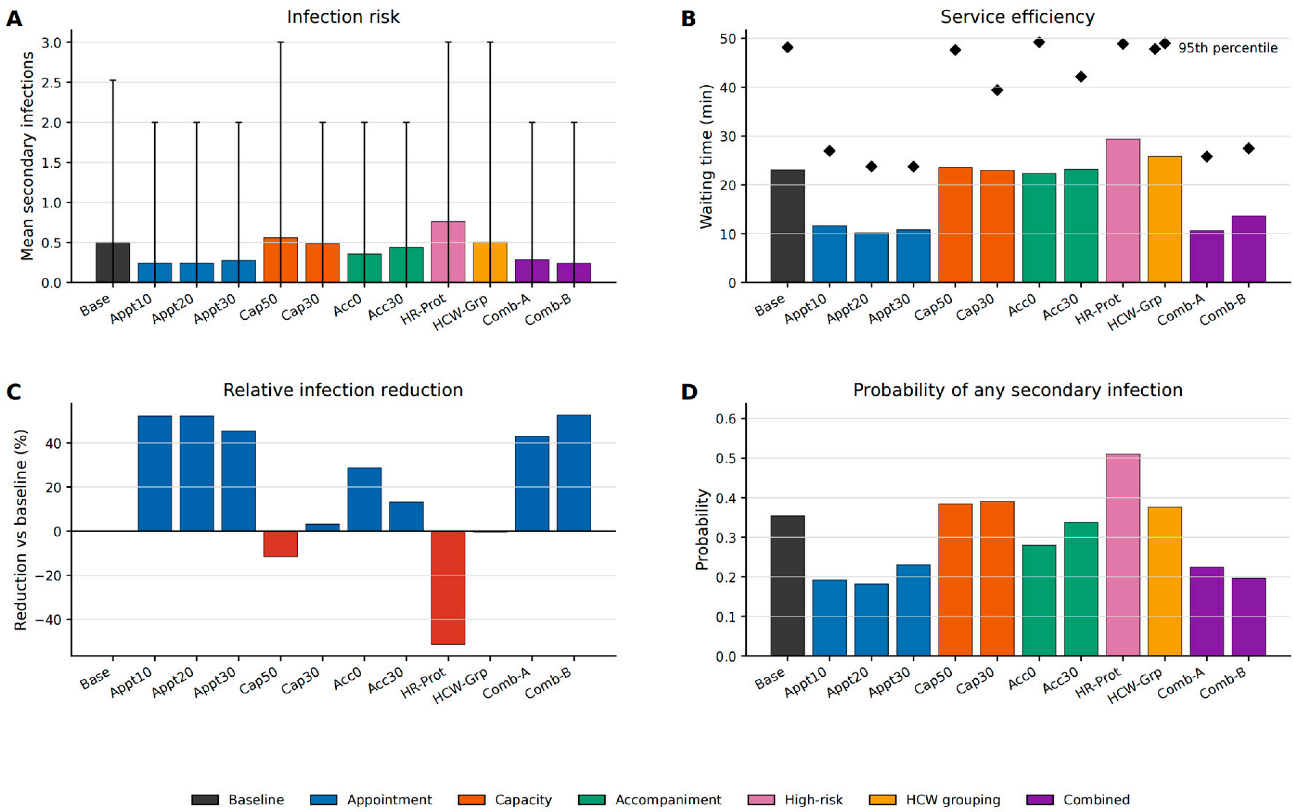

Figure 3. Scenario-level effects of outpatient flow-control policies on infection risk and service efficiency. (**A**) Mean cumulative secondary infections with observed simulation ranges. (**B**) Mean and 95th-percentile waiting times. (**C**) Relative reduction from baseline. (**D**) Probability of any secondary infection. Unless a scenario label changes a policy variable, Table 1 baseline parameters apply; R = 500 per scenario.

Appointment spacing also improved service efficiency. Mean waiting time decreased from 23.1 min under baseline to 11.6 min under Appt-10min, 10.2 min under Appt-20min, and 10.8 min under Appt-30min. The 95th percentile waiting time decreased from 48.2 min under baseline to 23.8 min under Appt-20min. Figure 3B shows these waiting-time outcomes. Under the present parameterization, appointment spacing therefore did not create a risk–efficiency trade-off; it reduced both simulated infection risk and waiting time by flattening arrival peaks and lowering waiting-room occupancy.

Waiting-capacity control showed more context-dependent effects. Capacity-50 increased mean secondary infections to 0.560, an 11.6% increase relative to baseline, whereas Capacity-30 produced 0.486 infections, a small reduction of 3.2%. This pattern indicates that capacity control is not automatically protective if it only displaces patients to another shared buffer or prolongs time in the facility. Capacity limits should therefore be interpreted as spatial-flow policies rather than simple contact-removal policies.

Accompaniment restriction produced a more consistent reduction in simulated infection risk. Removing accompanying persons reduced mean secondary infections to 0.358, a 28.7% reduction relative to baseline. Reducing accompaniment to 30% resulted in 0.436 mean infections, a 13.1% reduction. The mechanism is direct: fewer accompanying persons reduce the number of nodes and possible dyads in waiting and treatment zones. Figure 3D further shows that the probability of any secondary infection decreased under several flow-control strategies, particularly appointment spacing and the combined interventions. The combined scenarios are shown in Figure 3 for comparison, but their mechanisms are interpreted in Section 3.3.

3.3. Joint Policy Interactions and Combined Strategy Performance

The previous results showed that appointment spacing and accompaniment restriction were effective single operational strategies, whereas waiting-capacity control produced more context-dependent effects. To further examine how intervention effects depended on policy combinations, accompaniment-capacity interactions, protected scheduling for high-risk patients, healthcare-worker grouping, and combined strategies were compared. This analysis was necessary because outpatient infection-control policies rarely operate in isolation: a measure that reduces crowding in one zone may shift waiting burden elsewhere, and a measure designed to protect vulnerable patients may fail if it creates local concentration.

Figure 4 shows that accompaniment and waiting-capacity policies interacted in a non-monotonic way. Lower accompaniment did not always produce the lowest simulated infection risk, and stricter waiting-capacity limits did not consistently improve outcomes. For example, some low-capacity conditions increased waiting time without clearly reducing infections, suggesting that capacity control may redistribute contact burden rather than simply remove it. The paired heatmaps also show that infection risk and service efficiency need to be evaluated together. A policy combination with lower simulated infections can still be operationally undesirable if it substantially increases waiting time.

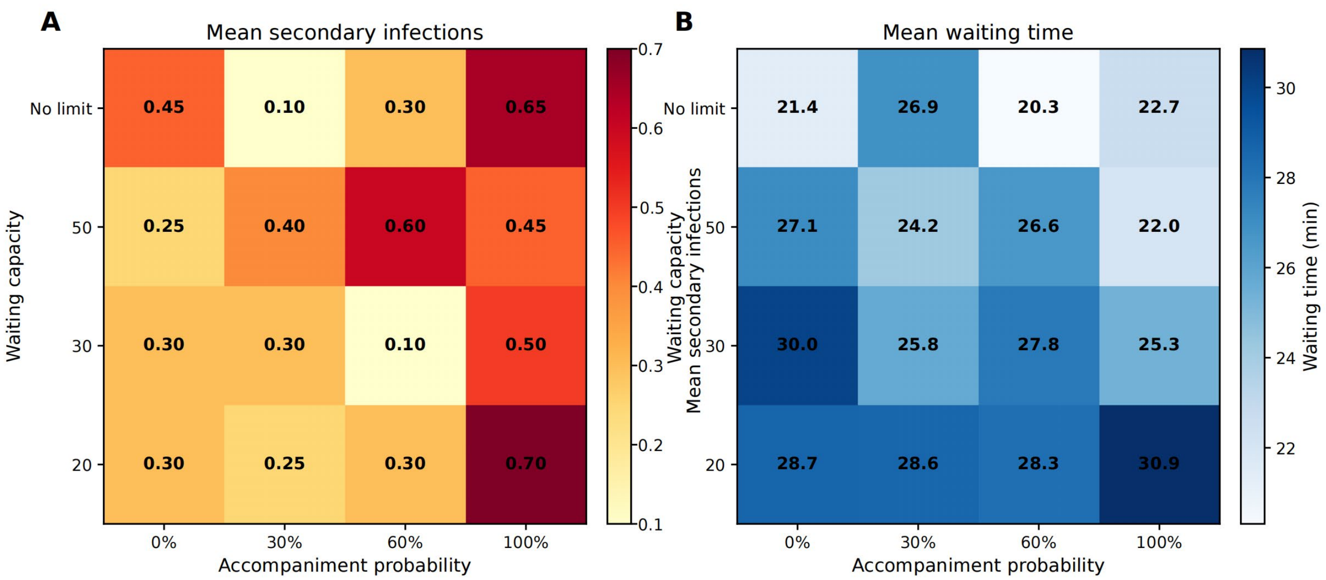

Figure 4. Joint effects of accompaniment ratio and waiting capacity. (**A**) Mean cumulative secondary infections. (**B**) Mean waiting time. All other parameters use Table 1 baseline values; R = 20 per grid cell.

Protected scheduling for high-risk patients also showed that targeted policies require careful process design. When implemented as a stand-alone early block, the high-risk protected scenario produced 0.760 mean secondary infections and a high-risk infection probability of 0.102, compared with 0.502 and 0.048 under baseline. The process metrics help explain this result: peak waiting occupancy increased to 64, and mean waiting time rose to 29.4 min. These findings indicate that time-based separation can create local concentration if it is not paired with density control and smooth patient flow. Therefore, the result should not be interpreted as evidence against protected scheduling itself, but as evidence that protected scheduling should be implemented as a low-density, well-managed pathway.

Figure 5A confirms that the stand-alone high-risk block increased high-risk infection probability, whereas the combined strategies reduced this probability to levels comparable with or lower than baseline. Combined-B produced a high-risk infection probability of 0.040, slightly below the baseline value of 0.048. Figure 5B shows that healthcare-worker grouping alone did not markedly reduce contact burden. Healthcare-worker grouping produced 0.504 mean secondary infections, almost unchanged from the baseline value, and increased mean waiting time to 25.8 min. The healthcare-worker bridge index was 0.785 under grouping, compared with 0.746 under baseline. This suggests that grouping may reduce some cross-zone movement, but it does not eliminate necessary patient–staff contacts and may reduce operational flexibility when demand is uneven across zones.

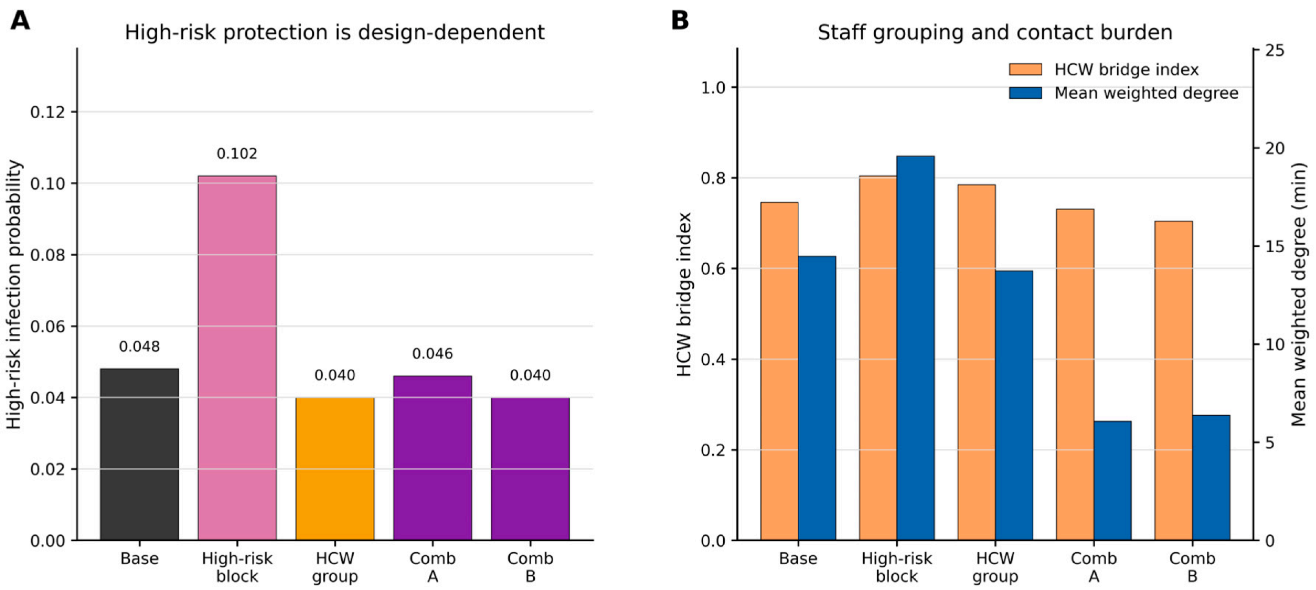

Figure 5. Targeted-protection and healthcare-worker bridging outcomes. (**A**) High-risk infection probability under different groups. (**B**) Healthcare-worker bridge index and mean weighted degree under different groups. Table 1 baseline values apply except for the named interventions; infection probabilities use R = 500.

Combined strategies performed better than most single strategies because they reduced contact opportunities without imposing large waiting penalties. Combined-A, which used time-spaced appointments and 30% accompaniment, reduced mean secondary infections to 0.286, corresponding to a 43.0% reduction relative to baseline, while keeping mean waiting time at 10.6 min. Combined-B, which included time-spaced appointments, capacity 30, 30% accompaniment, protected high-risk scheduling, and healthcare-worker grouping, produced the lowest mean secondary infections at 0.238, corresponding to a 52.6% reduction relative to baseline. Its probability of any secondary infection was 0.196, compared with 0.354 under baseline, and its mean waiting time was 13.6 min.

Figure 6 summarizes the overall comparison between single and combined strategies. Figure 6A shows that the most favourable strategies were not necessarily the most restrictive in every dimension. Appointment-based and combined strategies occupied the lower-left region of the plot, indicating lower simulated infection risk and shorter waiting time. By contrast, the stand-alone high-risk block had the highest infection risk and one of the longest waiting times, reinforcing the finding that targeted protection must be combined with density and flow management. Figure 6B shows the illustrative composite risk–efficiency–control score. The lowest scores were observed for appointment-based and combined strategies, whereas the high-risk block had the poorest score. The composite score is useful for summarizing policy performance, but infection risk, waiting time, and implementation burden should still be interpreted separately.

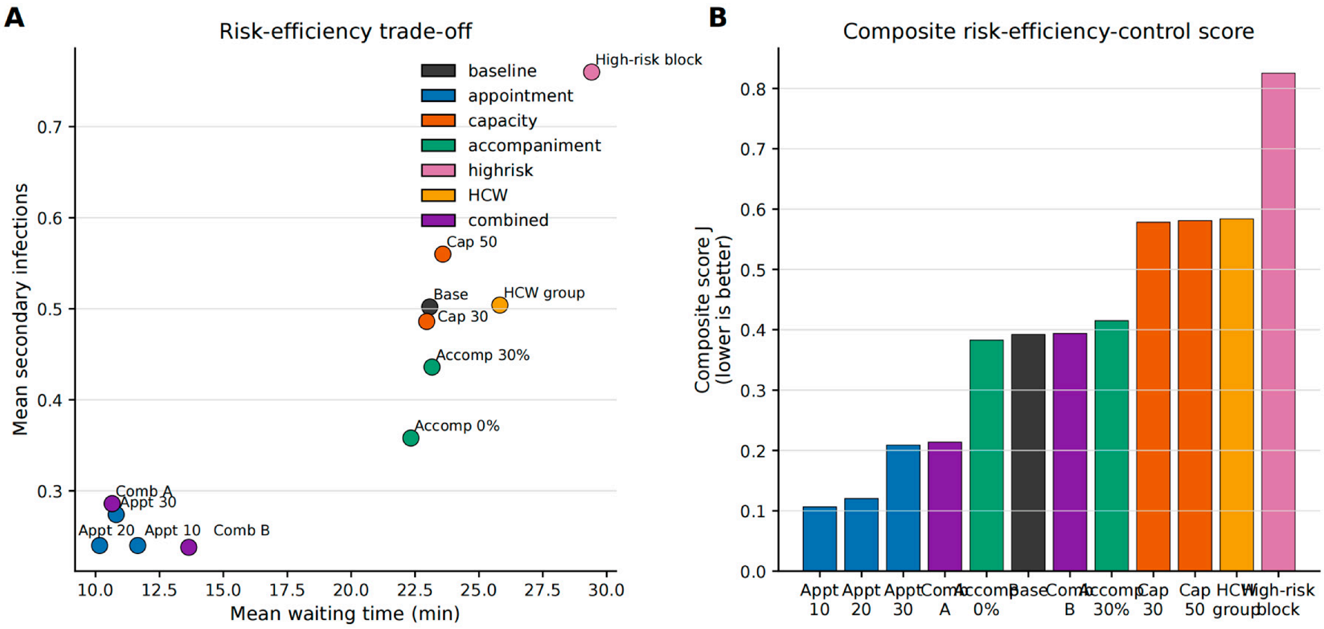

Figure 6. Risk–efficiency and composite policy comparison. (**A**) Mean secondary infections versus mean waiting time. (**B**) Composite score using min–max normalized infection and waiting outcomes, component-count control burden, and equal weights w1 = w2 = w3 = 1/3. Table 1 baseline values apply except for named interventions; R = 500.

Overall, these results show that outpatient infection-control strategies should be assessed as interacting operational designs rather than isolated rules. Appointment smoothing and accompaniment reduction acted directly on contact opportunities and performed consistently well. Capacity control, high-risk scheduling, and healthcare-worker grouping were more sensitive to implementation details. The best-performing combined strategies reduced simulated infection risk while maintaining acceptable waiting times, suggesting that coordinated flow management is more reliable than single targeted interventions.

3.4. Sensitivity of Infection Outcomes to Epidemiological and Operational Assumptions

To assess the robustness of the simulated infection outcomes under simultaneous parameter uncertainty, we conducted a multivariable Latin hypercube sampling analysis. This approach allowed epidemiological and operational inputs to vary jointly and enabled explicit evaluation of interaction effects that cannot be estimated using one-at-a-time sensitivity analysis. Particular attention was given to the interaction between the transmission rate β and waiting capacity because capacity restrictions may alter both the location and duration of potentially infectious contacts.

The multivariable Latin hypercube analysis evaluated 512 combinations of epidemiological and operational inputs. Across the LHS design, mean cumulative secondary infections ranged from 0.01 to 1.86 per clinic day, with a median of 0.305. The interaction-aware response surface explained 86.2% of the variation among design-point means, as shown in Table 3. The adjusted standardized $\beta \times$ waiting-capacity coefficient was 0.030 (95% bootstrap interval: -0.009 to 0.071), with partial $R^2 = 0.006$. In a complementary outer-tercile analysis, increasing capacity from the low category ($\leq$30 persons) to the high category ($\geq$40 persons) changed mean cumulative secondary infections by -0.020 in the low-β group and by -0.065 in the high-β group. The resulting difference-in-differences was -0.0446 infections (95% bootstrap interval: -0.1869 to 0.0988).

Table 3. Multivariable Latin hypercube sensitivity analysis. Standardized coefficients are from the interaction-aware response-surface models. The outer-tercile interaction is the difference-in-differences between high- and low-capacity contrasts under high and low β. Bootstrap intervals resampled the 512 LHS design points. Each design point used 100 stochastic epidemic replications.

Outcome	Response-Surface R^2	Standardized $\beta \times$ Capacity Coefficient (95% Bootstrap Interval)	Partial R^2	Outer-Tercile Interaction (95% Bootstrap Interval)
Mean cumulative secondary infections	0.862	0.030 (-0.009 to 0.071)	0.006	-0.0446 (-0.1869 to 0.0988)
Probability of any secondary infection	0.894	0.026 (-0.005 to 0.056)	0.006	-0.0167 (-0.0924 to 0.0590)

For the probability of any secondary infection, the response surface explained 89.4% of the variation among LHS points. The adjusted standardized $\beta \times$ waiting-capacity coefficient was 0.026 (95% bootstrap interval: -0.005 to 0.056; partial $R^2 = 0.006$). The corresponding outer-tercile difference-in-differences was -0.0167 probability units (95% bootstrap interval: -0.0924 to 0.0590). The continuous response-surface and outer-tercile interaction estimates differed in direction, and both bootstrap intervals included zero. We therefore found no stable $\beta \times$ waiting-capacity interaction within the evaluated ranges. Conditional parameter-group partial R^2 values for mean cumulative secondary infections were 0.753 for initial infectious count, 0.645 for β, 0.564 for arrival schedule, 0.187 for contact scaling, 0.112 for accompaniment probability, and 0.077 for waiting capacity. These values are not additive because interaction terms contribute to more than one parameter group.

These findings showed that initial infectious count, β, and arrival schedule were the dominant sources of variation, whereas the $\beta \times$ waiting-capacity interaction was comparatively small and uncertain. This result applies to the archived synthetic model and specified parameter ranges and should not be interpreted as evidence that the interaction will be absent in an empirically calibrated outpatient model.

4. Discussion

This study developed a synthetic contact-network simulation framework for outpatient infection-risk control. Its principal comparative finding is that outpatient flow organization can reshape temporal contact opportunities. Appointment spacing was the most consistent single strategy under the stated assumptions, while accompaniment restriction removed non-service nodes. Capacity control, protected scheduling, and healthcare-worker grouping were implementation-dependent. These are computational scenario findings, not clinical-effect estimates or universal recommendations.

The contact-matched homogeneous-mixing benchmark produced a similar order of magnitude but a higher expected baseline count than the temporal network. This comparison illustrates both roles of the network model: it provides a consistency check against aggregate mixing while retaining information about who meets whom, where, and when. Unlike prior healthcare network studies focused mainly on transmission over observed patient–staff contacts, the present model generates contacts from outpatient operational decisions. Its added value is therefore mechanism-level policy comparison, not an analytical stability proof or a replacement for empirical validation.

The appointment-spacing results suggest that temporal smoothing can reduce both infection risk and operational delay when arrival peaks are an important driver of contact burden. In the simulated scenarios, Appt-10min and Appt-20min reduced mean secondary infections by more than 50% relative to baseline and also shortened mean waiting time. This does not imply that longer or more widely spaced appointments are universally better. Real clinics face constraints in staffing, room availability, treatment duration, patient punctuality, emergency add-ons, and patient preferences. If appointment spacing reduces throughput or creates long idle periods, the operational trade-off may change. The model therefore supports studying appointment control as a joint infection-risk and service-efficiency problem rather than as a purely administrative scheduling task.

Capacity control was more nuanced because a numerical limit does not define physical separation. A lower-contact buffer is protective only if it is genuinely separated in space or time, has appropriate ventilation and supervision, and does not prolong sojourn. Priority pathways could instead use pre-entry check-in, direct rooming, separate waiting zones, or fast-track service for vulnerable patients. Future layout-aware models should represent room geometry, ventilation zones, corridor movement, and explicit adjacency so that "capacity" is not treated as a purely numerical intervention.

The accompaniment results are operationally important but require clinical caution. Removing or reducing accompanying persons decreased simulated infection risk because it reduced the number of nodes and possible contact pairs in waiting and treatment zones. However, the model should not be used to justify blanket restrictions. Accompanying persons may be essential for frail patients, paediatric patients, patients with cognitive impairment, patients with mobility limitations, or patients receiving complex treatment. A more practical policy implication is that accompaniment should be managed as a differentiated risk-control variable. Future models could assign accompaniment necessity by patient type and evaluate policies that preserve necessary support while limiting optional accompaniment during peak periods.

The high-risk scheduling result shows that a protective policy label is not sufficient to guarantee protection. In the simplified implementation, a stand-alone high-risk block increased simulated infection risk because it concentrated high-risk patients in an early period and increased local occupancy. This finding should not be interpreted as evidence against protected scheduling itself. Instead, it indicates that protection requires separation together with low density, adequate staffing, and smooth flow. A protected block that becomes crowded may not protect vulnerable patients. In contrast, the combined strategy that paired protected scheduling with appointment spacing, accompaniment reduction, capacity control, and healthcare-worker grouping produced lower high-risk infection probability than the stand-alone protected block. This illustrates the value of simulation before implementation: the effect of a policy depends on the process through which it is operationalized.

Healthcare-worker grouping also had limited stand-alone benefit in the present parameterization. This is plausible because outpatient care necessarily involves patient–staff contact. Reducing cross-zone staff movement may reduce some bridging opportunities, but it does not eliminate clinical contacts and may reduce flexibility when demand is uneven across zones. In the results, healthcare-worker grouping alone did not meaningfully reduce simulated infections and was associated with longer waiting time. This suggests that staff grouping should be coupled with appointment smoothing, workload balancing, and zone-level planning rather than used as an isolated intervention. Future versions should represent staff schedules more realistically, including breaks, room assignments, task types, and the difference between brief administrative contacts and close clinical contacts.

The global LHS analysis improves the assessment of multivariable effects and interactions, but it remains based on synthetic calibration and one operational/contact-network realization per LHS point. Its bootstrap intervals quantify design-point and Monte Carlo uncertainty rather than clinical sampling uncertainty. Site-specific prediction would require outpatient proximity or location data, timestamped appointments and services, layout and ventilation information, pathogen-specific parameters, empirical recalibration, and repetition of the global analysis using locally defensible parameter ranges.

The operational levers studied here are distinct from clinical infection-control measures. Appointment timing, routing, accompaniment, capacity, and staff zoning reshape contact opportunities; they do not replace screening, masks or respirators, ventilation, isolation, hand hygiene, environmental cleaning, vaccination, or clinical judgement. Combined strategies also create implementation burdens: scheduling may reduce flexibility, separated buffers require space and supervision, accompaniment exceptions require triage, and staff grouping can reduce workload balancing. Local adoption should therefore be co-designed by operations, infection-prevention, clinical, facilities, and patient-access teams.

Several limitations constrain the generalizability of these findings. All calibration records are synthetic: publicly available hospital-ward descriptions informed qualitative assumptions but did not validate the simulated outpatient contact network. The model also uses a generic respiratory-infection hazard, simplified service processes, and a one-day simulation horizon. It does not represent airborne transmission, ventilation, masking, vaccination, behavioural adaptation, no-shows, urgent add-on visits, environmental cleaning, room geometry, or multi-day transmission. Although the multivariable Latin hypercube analysis evaluates parameter interactions, it remains based on synthetic calibration and one operational contact-network realization per design point; its bootstrap intervals therefore quantify simulation and design uncertainty rather than clinical sampling uncertainty. Site-specific prediction would require outpatient proximity or location data, timestamped appointment and service records, facility-layout and ventilation information, pathogen-specific parameters, empirical recalibration, locally defined uncertainty ranges, and prospective validation.

Despite these limitations, the framework is useful because it separates empirical, methodological, and practical claims. The empirical claim is that outpatient temporal contact data are needed to measure real contact structures; the present version does not claim to provide such observed outpatient data. The methodological claim is that dynamic contact-network simulation can connect outpatient organization to infection risk; the present study implements this link. The practical claim is that operational policies can reduce or shift contact risk; the present results support this claim under the stated assumptions but do not identify a universal policy.

The modular design of the simulation framework is also important. Outpatient infection control is not a single-parameter problem. A clinic manager may be able to adjust appointment spacing but not increase the number of rooms. A clinical team may reduce optional accompaniment but must preserve support for patients who need assistance. Infection-control staff may recommend cohorting or screening, but these

https://doi.org/10.3390/math14163021

interventions can alter waiting time, workload, and contact displacement. By separating process generation, temporal contact construction, and stochastic transmission, the framework allows each assumption to be inspected, replaced, and recalibrated. For example, electronic appointment timestamps could update arrival distributions, proximity sensors could update contact probabilities, and electronic health records could update treatment-duration distributions.

Future research should collect outpatient temporal contact data with role labels, zone labels, and appointment timestamps. Such data would allow direct estimation of zone-specific contact probabilities, contact-duration distributions, high-contact-node concentration, and healthcare-worker bridge roles. Future models should also incorporate pathogen-specific parameters, patient-level susceptibility, vaccination status, ventilation and room size, mask adherence, and multi-day transmission. Finally, optimization methods could be added to search over appointment templates, staffing patterns, capacity rules, and accompaniment exceptions subject to clinical constraints.

5. Conclusions

This study presents a transparent synthetic contact-network simulation framework linking outpatient processes, temporal contacts, stochastic SEIR transmission, and risk–efficiency comparison. Under the stated assumptions, appointment spacing and accompaniment reduction lowered simulated risk, whereas capacity control, protected scheduling, and staff grouping depended on implementation. These results neither predict infections in a named clinic nor establish universal clinical policy. They identify testable operational mechanisms and a workflow that can be recalibrated and validated with local outpatient data before decision use.

Author Contributions: Conceptualization, R.F. and Z.Z.; Methodology, R.F. and Z.Z.; Software, Y.T.; Validation, Z.Z., H.J. and Y.T.; Formal analysis, Y.T.; Investigation, H.J.; Resources, H.J.; Data curation, Y.T.; Writing—original draft, R.F.; Writing—review & editing, R.F., Z.Z., H.J. and Y.T.; Visualization, Y.T.; Supervision, R.F.; Project administration, R.F. and Y.T. All authors have read and agreed to the published version of the manuscript.

Funding: This research received no external funding.

Institutional Review Board Statement: Not applicable, because this study used simulated data and synthetic calibration data and did not involve human participants.

Informed Consent Statement: Not applicable.

Data Availability Statement: The synthetic data and simulation code generated in this study are publicly available in Zenodo at https://doi.org/10.5281/zenodo.21952193 (accessed on 14 August 2026).

Conflicts of Interest: The authors declare no conflicts of interest.

References

1. Weston, D.; Burgess, A.; Roberts, S. *Infection Prevention and Control at a Glance*; John Wiley & Sons: Hoboken, NJ, USA, 2016.
2. Damani, N. *Manual of Infection Prevention and Control*; Oxford University Press: Oxford, UK, 2019.
3. World Health Organization (Ed.) *Infection Prevention and Control in the Context of COVID-19: A Guideline*; World Health Organization: Geneva, Switzerland, 2023.
4. Kermack, W.O.; McKendrick, A.G. A Contribution to the Mathematical Theory of Epidemics. *Proc. R. Soc. Lond. Ser. Contain. Pap. Math. Phys. Character* **1927**, *115*, 700–721. [CrossRef]
5. Keeling, M.J.; Eames, K.T. Networks and Epidemic Models. *J. R. Soc. Interface* **2005**, *2*, 295–307. [CrossRef] [PubMed]
6. Danon, L.; Ford, A.P.; House, T.; Jewell, C.P.; Keeling, M.J.; Roberts, G.O.; Ross, J.V.; Vernon, M.C. Networks and the Epidemiology of Infectious Disease. *Interdiscip. Perspect. Infect. Dis.* **2011**, *2011*, 284909. [CrossRef] [PubMed]
7. Pastor-Satorras, R.; Castellano, C.; Van Mieghem, P.; Vespignani, A. Epidemic Processes in Complex Networks. *Rev. Mod. Phys.* **2015**, *87*, 925–979. [CrossRef]

8. Holme, P.; Saramäki, J. Temporal Networks. *Phys. Rep.* **2012**, *519*, 97–125. [CrossRef]
9. Cattuto, C.; Van den Broeck, W.; Barrat, A.; Colizza, V.; Pinton, J.-F.; Vespignani, A. Dynamics of Person-to-Person Interactions from Distributed RFID Sensor Networks. *PLoS ONE* **2010**, *5*, e11596. [CrossRef] [PubMed]
10. Salathé, M.; Kazandjieva, M.; Lee, J.W.; Levis, P.; Feldman, M.W.; Jones, J.H. A High-Resolution Human Contact Network for Infectious Disease Transmission. *Proc. Natl. Acad. Sci. USA* **2010**, *107*, 22020–22025. [CrossRef] [PubMed]
11. Stehlé, J.; Voirin, N.; Barrat, A.; Cattuto, C.; Isella, L.; Pinton, J.-F.; Quaggiotto, M.; Van den Broeck, W.; Régis, C.; Lina, B. High-Resolution Measurements of Face-to-Face Contact Patterns in a Primary School. *PLoS ONE* **2011**, *6*, e23176. [CrossRef] [PubMed]
12. Vanhems, P.; Barrat, A.; Cattuto, C.; Pinton, J.-F.; Khanafer, N.; Régis, C.; Kim, B.; Comte, B.; Voirin, N. Estimating Potential Infection Transmission Routes in Hospital Wards Using Wearable Proximity Sensors. *PLoS ONE* **2013**, *8*, e73970. [CrossRef] [PubMed]
13. Yuan, Z.; Lin, S.; Mao, Z.; Xie, C.; Tong, Y.; Li, Y.; Jia, H. Evaluating Underground Space of Rail Transit Hub Evacuation under Fire Scenarios: Virtual Reality Meets Agent-Based Simulation. *Accid. Anal. Prev.* **2026**, *228*, 108389. [CrossRef] [PubMed]
14. Ma, Y.; Yu, M.; Zhang, H.; Tong, Y.; Gou, J.; Huo, F. Guided Evacuation Simulation of Panic-Driven Heterogeneous Pedestrians in Multi-Exits Building. *J. Build. Eng.* **2025**, *108*, 112873. [CrossRef]
15. Tong, Y.; Bode, N.W.; Haghani, M.; Lovreglio, R. Exploring Occupant Exit Choices during Fire Drills and False Alarm Evacuations in a Library. *Saf. Sci.* **2025**, *182*, 106708. [CrossRef]
16. Voirin, N.; Payet, C.; Barrat, A.; Cattuto, C.; Khanafer, N.; Régis, C.; Kim, B.; Comte, B.; Casalegno, J.-S.; Lina, B.; et al. Combining High-Resolution Contact Data with Virological Data to Investigate Influenza Transmission in a Tertiary Care Hospital. *Infect. Control Hosp. Epidemiol.* **2015**, *36*, 254–260. [CrossRef] [PubMed]
17. Pham, T.M.; Tahir, H.; van de Wijgert, J.H.; Van der Roest, B.R.; Ellerbroek, P.; Bonten, M.J.; Bootsma, M.C.; Kretzschmar, M.E. Interventions to Control Nosocomial Transmission of SARS-CoV-2: A Modelling Study. *BMC Med.* **2021**, *19*, 211. [CrossRef] [PubMed]
18. Myall, A.; Price, J.R.; Peach, R.L.; Abbas, M.; Mookerjee, S.; Zhu, N.; Ahmad, I.; Ming, D.; Ramzan, F.; Teixeira, D.; et al. Prediction of Hospital-Onset COVID-19 Infections Using Dynamic Networks of Patient Contact: An International Retrospective Cohort Study. *Lancet Digit. Health* **2022**, *4*, e573–e583. [CrossRef] [PubMed]
19. Smith, D.R.; Chervet, S.; Pinettes, T.; Shirreff, G.; Jijón, S.; Oodally, A.; Jean, K.; Opatowski, L.; Kernéis, S.; Temime, L. How Have Mathematical Models Contributed to Understanding the Transmission and Control of SARS-CoV-2 in Healthcare Settings? A Systematic Search and Review. *J. Hosp. Infect.* **2023**, *141*, 132–141. [CrossRef] [PubMed]
20. Pujante-Otalora, L.; Canovas-Segura, B.; Campos, M.; Juarez, J.M. The Use of Networks in Spatial and Temporal Computational Models for Outbreak Spread in Epidemiology: A Systematic Review. *J. Biomed. Inform.* **2023**, *143*, 104422. [CrossRef] [PubMed]
21. Cayirli, T.; Veral, E. Outpatient Scheduling in Health Care: A Review of Literature. *Prod. Oper. Manag.* **2003**, *12*, 519–549. [CrossRef]
22. Gupta, D.; Denton, B. Appointment Scheduling in Health Care: Challenges and Opportunities. *IIE Trans.* **2008**, *40*, 800–819. [CrossRef]
23. Ahmadi-Javid, A.; Jalali, Z.; Klassen, K.J. Outpatient Appointment Systems in Healthcare: A Review of Optimization Studies. *Eur. J. Oper. Res.* **2017**, *258*, 3–34. [CrossRef]
24. Comis, M.; Cleophas, C.; Büsing, C. Patients, Primary Care, and Policy: Agent-Based Simulation Modeling for Health Care Decision Support. *Health Care Manag. Sci.* **2021**, *24*, 799–826. [CrossRef] [PubMed]
25. Kuiper, A.; de Mast, J.; Mandjes, M. The Problem of Appointment Scheduling in Outpatient Clinics: A Multiple Case Study of Clinical Practice. *Omega* **2021**, *98*, 102122. [CrossRef]